

Generation and characterization of quasi-monoenergetic electron beams from laser wakefield

A. Maksimchuk¹, S. Reed¹, N. Naumova¹, V. Chvykov¹, B. Hou¹,
G. Kalintchenko¹, T. Matsuoka¹, J. Nees¹, P. Rousseau¹, G. Mourou¹
and V. Yanovsky¹

¹ *FOCUS Center and Center for Ultrafast Optical Science, University of Michigan,
2200 Bonisteel Blvd., Ann Arbor, Michigan 48109, USA*

Abstract. In the interaction of a 30 fs, 40 TW Ti:sapphire Hercules laser focused to the intensity of 10^{19} W/cm² onto a supersonic He gas jet, we observed quasi-monoenergetic electron beams with energy up to 300 MeV and an angular divergence of 10 mrad. We found that the initial plasma density significantly affects the resultant electron beam. For plasma densities ranging between 2×10^{19} to 3.5×10^{19} cm⁻³, quasi-monoenergetic electrons with energies from 80 to 160 MeV and a total charge of about 0.5 nC were produced. Lower plasma densities around 1.5×10^{19} cm⁻³ produced quasi-monoenergetic electron beams with higher energy, up to 320 ± 50 MeV, but with a decrease of the total charge to about 5 pC. Characterization of the electron beam in terms of the electron's maximum energy, beam divergence and pointing stability is presented. The performed 2D PIC simulations show the evolution of the laser pulse in the plasma, electron injection, and the specifics of electron acceleration.

1. INTRODUCTION

Laser-driven plasma wakefield accelerators have the potential to become the next generation of particle accelerators [1] because of the very high acceleration gradients reaching several hundreds of GV/m. These fields are thousands of times greater than those in the conventional radio-frequency linacs making plasma wakefield accelerators a promising compact ultrashort source of electrons, x-rays, and gamma radiation. In the last decade, most studies have concentrated on electron beams generated from self-modulated laser wakefield accelerators (SM-LWFA) [2, 3] and more recently from the forced laser wakefield (F-LWFA) accelerators [4]. Both of these accelerators produce an exponential electron energy spectrum with a relatively small number of electrons near the maximum energy of around 200 MeV. For many applications monochromatic electron beams are required. Recent developments in short-pulse lasers based on Ti:Sapphire technology routinely allow for laser pulses with power exceeding tens of terawatts, with pulse durations less than 50 fs at 10 Hz repetition rates. Using such lasers three groups [5-7] reported the production of quasi-monoenergetic electron beams with a maximum energy up to 170 MeV. In this paper we present a detailed study on the characterization of laser-wakefield accelerated electrons from plasma with density a few times higher than the resonant density and demonstrate the generation of quasi-monoenergetic electrons with energy up to 300 MeV with an exceptionally small divergence and beam pointing stability.

2. EXPERIMENTAL SETUP

The experiments have been performed with the 40 TW, 30 fs Ti:Sapphire CPA Hercules laser at the University of Michigan. The 75 mm diameter laser beam was focused with a 1 meter focal distance parabolic mirror onto the edge of a 2-mm-diameter supersonic He jet nozzle providing up to 10^{19} W/cm² intensity. The electron beam spatial distribution was measured using a LANEX phosphor screen imaged onto a CCD. An integrating current transformer (ICT) was used to measure the electron beams

total current. The electron energy spectrum was measured using a dipole magnetic spectrometer with detection on a phosphor screen. The dynamics of the laser-plasma interaction was monitored using a modified Mach-Zehnder interferometer with a variable delay line. The electron density of the gas jet has been reconstructed by processing the interferograms. Additionally, we monitored the laser light transmitted through the plasma of the gas jet by imaging the exit of the nozzle with ~ 5 micron resolution.

3. EXPERIMENTAL RESULTS

We observed a narrow beam of electrons with a divergence of about 10 mrad for electron densities between 1.5×10^{19} and $3 \times 10^{19} \text{ cm}^{-3}$ (Fig. 1a). Higher plasma densities lead to larger diameter electron beams (Fig. 1b) and even to the beam break up. The pointing stability is strongly dependent on the electron density as well. It was found that the lower densities lead to more directional beams. At densities of 1.5×10^{19} to $2 \times 10^{19} \text{ cm}^{-3}$, beam pointing fluctuations were 20 mrad which is only a small fraction of the laser beam cone (Fig. 1c). Measurements of the electron beam charge using an ICT and x-ray film showed that approximately 0.5 nC is contained in the beam for plasma electron densities between 2×10^{19} and $4 \times 10^{19} \text{ cm}^{-3}$ compared to densities below $2 \times 10^{19} \text{ cm}^{-3}$ which produced beams of about 2 orders of magnitude lower charge.

We performed a spectroscopy of resultant electron beams using a dipole magnet with a 0.8 mm slit in front of it. This setup allows for an improved spectral resolution in the electron momentum measurements, especially for the higher electron energies and when shot-to-shot angular fluctuations of the electron beam are comparable or larger than the angular divergence of the beam itself. We found that in the above density range the electron spectra are not Maxwellian and show a multiple peak structure at high energies. Many laser shots show that only two or even one peak in the spectrum can be produced (Fig. 2a,b). We observe that the maximum electron energy depends on a density of the gas jet. For higher plasma densities the maximum electron energies are typically lower with a shot-to-shot change ranging in average maximum energy from 70 to 120 MeV for densities ranging between 4×10^{19} to $2 \times 10^{19} \text{ cm}^{-3}$. When the electron density is below $2 \times 10^{19} \text{ cm}^{-3}$ we observe a further increase in the maximum electron energy up to 320 ± 50 MeV. In this case the number of accelerated electrons is significantly reduced.

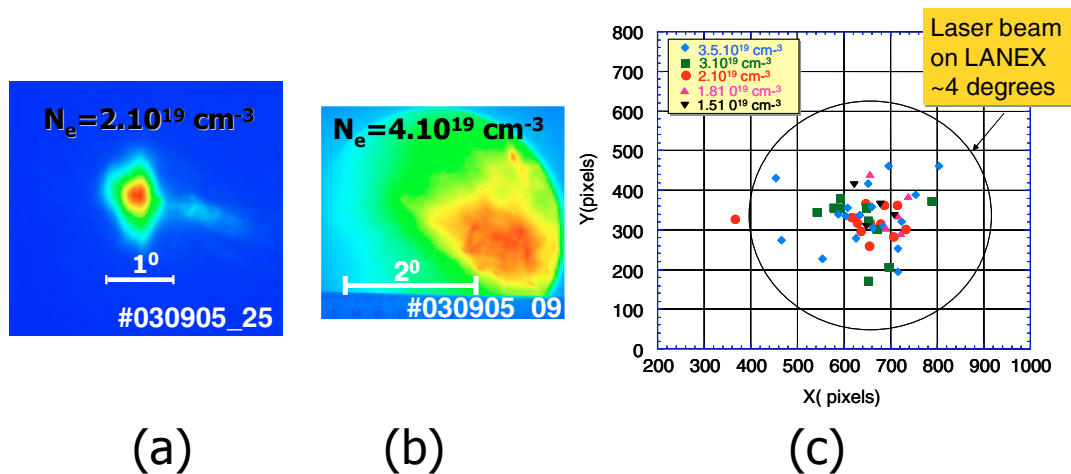


Figure 1. Images of the electrons on the LANEX screen for electron density of $2 \times 10^{19} \text{ cm}^{-3}$ (a) and $3.5 \times 10^{19} \text{ cm}^{-3}$. Beam pointing stability for electron densities ranging from $1.5 \times 10^{19} \text{ cm}^{-3}$ to $3.5 \times 10^{19} \text{ cm}^{-3}$. The circle indicates the size of the laser beam on the phosphor screen.

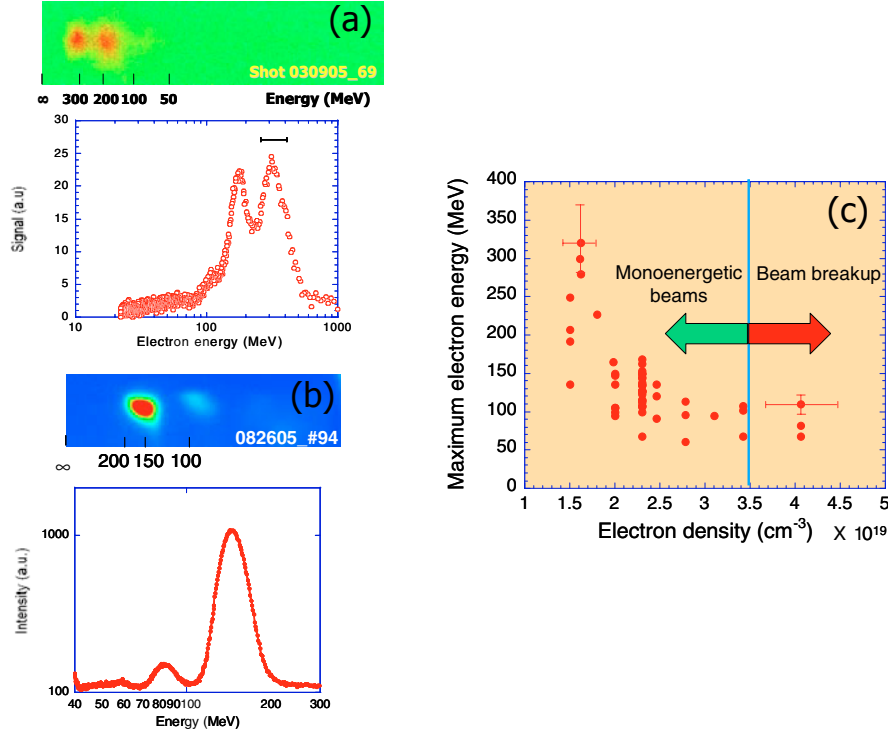


Figure 2. Measured electron spectrum and lineout at $n_e = 1.5 \times 10^{19} \text{ cm}^{-3}$ which demonstrates a double peak structure with a maximum energy of $320 \pm 50 \text{ MeV}$ (a); electron spectrum and lineout at $n_e = 2.5 \times 10^{19} \text{ cm}^{-3}$ with a maximum energy of $145 \pm 15 \text{ MeV}$ (b) and the dependence of the maximum electron versus plasma electron density (c).

4. RESULTS OF PIC SIMULATIONS AND DISCUSSION

To demonstrate the acceleration process for laser-plasma parameters close to the experimental conditions, we performed 2D particle-in-cell (PIC) simulations. In Fig. 3 the simulation results for a linear polarized laser pulse with amplitude of $a_0 = 2$, interacting with a plasma slab with a density $n = (1/10)^2 n_{cr}$ are shown. Spatial coordinates are measured in units of laser wavelength, and time is measured in optical cycles. This simulation was performed in the moving frame with a spatial size of 120×100 .

The bunch formation process due to the transverse wave-breaking [8] is demonstrated in Fig. 3. Electrons at the end of the first cycle, acquiring energy, which exceeds the critical value, become trapped in the favorite phase of the electric field. There is a high probably of electron trapping because of the laser beam self-focusing and pulse shortening, which leads to the change of the pulse intensity, and consequently, to a longer wakefield wavelength and higher wakefield amplitude. These trapped electrons are accelerated to higher energies, while simultaneously loading the wakefield, thus leading to the reduction of the wakefield amplitude behind them. As a result, the trapping process stops and the bunch becomes confined in space and further accelerated. The trends observed in the experiment can be explained by the interplay of self-focusing, dephasing and beam loading. For higher plasma densities the wakefield amplitude is higher, however, the dephasing distance $L_{dph} = \lambda_p^3 / \lambda_0^2$ becomes shorter. High-energy electrons propagating in plasma with the length greater than L_{dph} may lose their energy (Fig.3b,c) by outrunning the plasma wave and by going into the deceleration stage. For $n_e = 1.5 \times 10^{19} \text{ cm}^{-3}$ the dephasing length is about 1 mm and comparable with the size of the nozzle L_0 , while for plasma with

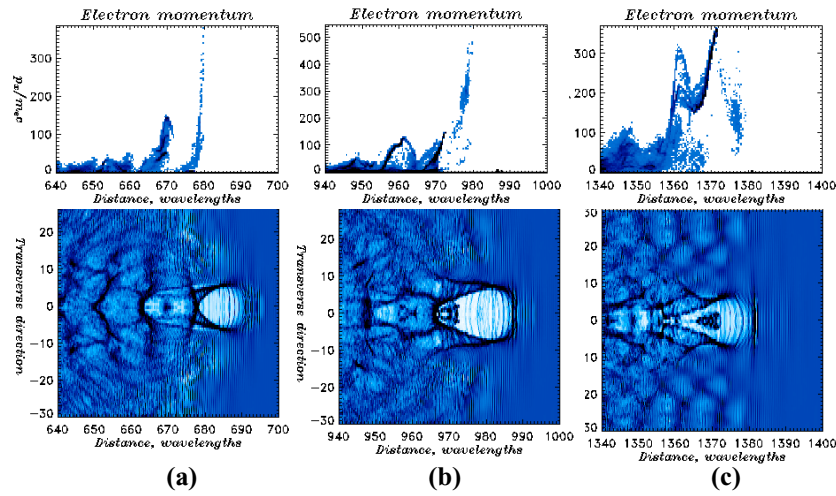


Figure 3. Generation of quasi-monoenergetic electron bunches. Electron density (upper pictures) and energy distribution of electrons (lower pictures) at three time instants. Parameters of 2D PIC simulation: $\tau = 30$ fs, $\lambda = 0.8 \mu\text{m}$, $d = 20 \lambda$, $I = 6 \times 10^{18} \text{ W/cm}^2$, $n_0 = 2 \times 10^{19} \text{ cm}^{-3}$ ($a = eE/m\omega_0 c = 2$; $\omega_0/\omega_p = 10$).

$n_e = 3.5 \times 10^{19} \text{ cm}^{-3}$, $L_{dph} = 0.27 \text{ mm}$ is much shorter than L_0 . This may explain the experimentally observed reduction in electron energy for higher plasma densities. Laser light transmitted through the plasma and detected with the mode imaging system shows that for lower plasma densities relativistic self-focusing is less efficient. This may lead to lower intensities in the plasma channel, smaller amplitude of the plasma wave, reduced trapping efficiency and to a smaller number of high-energy electrons in the beam.

Acknowledgments

This work was supported by the NSF through the Physics Frontier Center FOCUS. Part of the experimental equipment was supported by DOE. T. M. acknowledges the support from the Japanese Society for the Promotion of Science. The authors appreciate contributions from R. Shah, S. Banerjee, D. Umstadter, G. Sarkisov and N. Matlis.

References

- [1] T. Tajima and J. M. Dawson, *Phys. Rev. Lett.* **43**, 267 (1979).
- [2] A. Modena et al., *Nature* **337**, 606 (1995).
- [3] D. Umstadter et al., *Science* **273**, 472 (1996).
- [4] V. Malka et al., *Science* **298**, 1600 (2002).
- [5] J. Faure et al., *Nature* **431**, 541 (2004).
- [6] C. G. Geddes et al., *Nature* **431**, 538 (2004).
- [7] S. P. D. Mangles et al., *Nature* **431**, 535 (2004).
- [8] S. V. Bulanov et al., *Phys. Rev. Lett.* **78**, 4205 (1995).